Organometallics **1998,** *17,* 3648−3655

Articles

Preparation of N,N′-Disilylated 1,8-Diaminonaphthalene Chelates and Their Group 4 Metal Complexes for Ethylene Polymerization

Choong Hoon Lee, Young-Hye La, Soo Jin Park, and Joon Won Park*

Department of Chemistry, Center for Biofunctional Molecules, Pohang University of Science and Technology, San 31 Hyoja-dong, Pohang, 790-784, Korea

Received March 16, 1998

The reaction of 1,8-diaminonaphthalene with trimethylchlorosilane and tri(isopropyl)-chlorosilane gives N,N′-disilylated products (**1a**,**b**) in moderate yields. Double deprotonation of **1a**,**b** with *n*-BuLi yields the dilithiated products (**2a**,**b**) in 78−85% yield. The reaction of **2a**,**b** with $TiCl_4$ produces diamidotitanium(IV) dichlorides, $\{1,8\text{-}C_{10}H_6(NSiMe_3)_2\}TiCl_2$ (**3a**) and $\{1,8\text{-}C_{10}H_6(NSi(i\text{-}Pr)_3)_2\}TiCl_2$ (**3b**). The crystal structure of **3a** shows that the complex has an unusually large Cl−Ti−Cl angle (120.5°). Meanwhile, the bulkier substituents on the nitrogen atoms of **3b** are significantly away from the naphthalene plane. The reaction of **2a**,**b** with $ZrCl_4$ produces a bis(diamido)zirconium(IV) complex $\{1,8\text{-}C_{10}H_6(NSiMe_3)_2\}_2Zr$ (**4a**) and a diamidozirconium(IV) dichloride $\{1,8\text{-}C_{10}H_6(NSi(i\text{-}Pr)_3)_2\}ZrCl_2$ (**4b**), respectively. The crystal structure of **4b** shows that the molecule forms a dimer associated through two chloro bridges in the solid state. Facile monomethylation and transmetalation of **3a** to form a dinuclear aluminum complex (**5**) were observed when it was exposed to trimethylaluminum. The molecular structure of **5** is identified with an independent synthesis and X-ray crystallography. The crystal structure of **5** shows that two nitrogen centers and two aluminum centers comprise a metallacycle in a butterfly shape. In contrast, only monomethylation of **3b** occurs at room temperature. However, no sign of methylation was observed for **4b** at all. With a modified methylalumoxane (MAO), transfer of methyl and isopropyl groups to **3a** and **3b** was observed at room temperature. However, the transmetalated product **5** was not observed under the particular conditions. It is found that **3a** and **3b** show the marginal reactivity for ethylene polymerization in the presence of MAO.

Introduction

Since the constrained-geometry catalyst was reported recently,[1,2] several new types of early transition metal complexes having diamido[3] or dialkoxo[4] chelate ligands have been studied for homogeneous Ziegler−Natta polymerization. Chelate ligands of the new types provide characteristic electronic and geometrical environments, while maintaining the desirable catalytic activity. In particular, $[RN(CH_2)_3NR]TiMe_2$ (R = aryl)[3e,f] and $[((t\text{-Bu})N\text{-}o\text{-}C_6H_4)_2O]ZrMe_2$[3g] are found to be highly active living polymerization catalysts for even higher α-olefins. Herein we would like to present characteristic behavior of titanium(IV) and zirconium(IV) complexes having a rigid diamido ligand.

Experimental Section

General Procedure. All manipulations of air- and/or moisture-sensitive compounds were carried out with use of

---

[1] (a) Shapiro, P. J.; Bunel, E.; Schaefer, W. P.; Bercaw, J. E. *Organometallics* **1990**, *9*, 867. (b) Stevens, J. C.; Timmers, F. J.; Wilson, D. R.; Schmidt, G. F.; Nickias, P. N.; Rosen, R. K.; Knight, G. W.; Lia, S.-Y. (Dow Chemical Company). Eur. Pat. Appl. 0146 815 A2, 1990. (c) Canich, J. A. M. (Exxon). U.S. Patent 5,026,798, 1991.

[2] For recent reports: (a) Schwink, L.; Knochel, P.; Eberle, T.; Okuda, J. *Organometallics* **1998**, *17*, 7. (b) Chen, Y.-X.; Marks, T. J. *Organometallics* **1997**, *16*, 3649. (c) McKnight, A. L.; Masood, M. A.; Waymouth, R. M.; Straus, D. A. *Organometallics* **1997**, *16*, 2879. (d) Sinnema, P.-J.; van der Veen, L.; Spek, A. L.; Veldman, N.; Teuben, J. H. *Organometallics* **1997**, *16*, 4245. (e) Carpenetti, D. W.; Kloppenburg, L.; Kupec, J. T.; Peterson, J. L. *Organometallics* **1996**, *15*, 1572.

[3] For polymerization using group 4 metal chelating diamido complexes: (a) Warren, T. H.; Schrock, R. R.; Davis, W. M. *Organometallics* **1998**, *17*, 308. (b) Schrock, R. R.; Schattenmann, F.; Aizenberg, M.; Davis, W. M. *J. Chem. Soc., Chem. Commun.* **1998**, 199. (c) Gibson, V. C.; Kimberley, B. S.; White, A. J. P.; Williams, D. J.; Howard, P. *J. Chem. Soc., Chem. Commun.* **1998**, 313. (d) Male, N. A. H.; Thornton-Pett, M.; Bochmann, M. *J. Chem. Soc., Dalton Trans.* **1997**, 2487. (e) Scollard, J. D.; McConville, D. H. *J. Am. Chem. Soc.* **1996**, *118*, 10008. (f) Scollard, J. D.; McConville, D. H.; Vittal, J. J. *Macromolecules* **1996**, *29*, 5241. (g) Baumann, R.; Davis, W. M.; Schrock, R. R. *J. Am. Chem. Soc.* **1997**, *119*, 3830. (h) Tinkler, S.; Deeth, R. J.; Duncalf, D.; McCamley, A. *J. Chem. Soc., Chem. Commun.* **1996**. 2623. (i) Horton, A. D.; de With, J.; van der Linden, A. J.; van der Weg, H. *Organometallics* **1996**, *15*, 2672. (j) Cloke, F. G. N.; Geldbach, T. J.; Hitchcock, P. B.; Love, J. B. *J. Organomet. Chem.* **1996**, *506*, 343. (k) Scollard, J. D.; McConville, D. H.; Vittal, J. J. *Organometallics* **1997**, *16*, 4415. (l) Armistead, L. T.; White, P. S.; Gagné, M. R. *Organometallics* **1998**, *17*, 216.

[4] (a) van der Linden, A.; Schaverien, C. J.; Meijboom, N.; Ganter, C.; Orpen, A. G. *J. Am. Chem. Soc.* **1995**, *117*, 3008. (b) Fokken, S.; Spaniol, T. P.; Okuda, J. *Organometallics* **1997**, *16*, 4240.

S0276-7333(98)00187-3 CCC: $15.00

standard Schlenk or vacuum-line techniques. Argon was purified by being passed through columns of Ridox oxygen scavenger (R31-3, Fisher) and Linde 4 Å molecular sieves. Solids were transferred and stored in an N_2-filled Vacuum Atmospheres glovebox equipped with a HE-493 Dri-Train, a CS-40 Dri-Cold, and an oxygen analyzer (Model 315, Teledyne Analytical Instruments).

Anhydrous toluene, tetrahydrofuran, and diethyl ether were purchased from Aldrich and transferred to a sodium/benzophenone ketyl without prior treatment. Hexane and pentane were stirred over concentrated H_2SO_4, dried over CaH_2, and then transferred to a sodium/benzophenone ketyl. Dried deoxygenated solvents were vacuum-transferred to dry glass vessels equipped with a J-Young valve and stored under argon. Benzene-d_6, toluene-d_8, and THF-d_8 were transferred from purple sodium/benzophenone ketyl. 1,8-Diaminonaphthalene, $ClSiMe_3$, $ClSi(i\text{-}Pr)_3$, *n*-BuLi (1.6 M in hexane), $TiCl_4$ (1.0 M in toluene), $ZrCl_4$, ethylene (99.5+%), and $AlMe_3$ were used as received from Aldrich. Methylalumoxane (Akzo, type 4) modified with isobutyl group was purchased as a toluene solution, and the solid alumoxane was obtained by evaporating the solvent in vacuum at room temperature for 24 h.

NMR spectra were recorded on Bruker DRX500 (500 MHz, ^1H) and DPX300 (300 MHz, ^1H) spectrometers. Chemical shifts are reported in δ, referenced to residual solvent signals. GPC measurements were carried out using a PL-GPC 210 instrument (Shodex AT-806 MS columns). Elemental analyses were performed at either Galbraith Laboratories, Inc., or Pohang University of Science and Technology (Elementar Vario-EL).

Synthesis of 1,8-$C_{10}H_6(NHSiMe_3)_2$ (1a). 1,8-Diaminonaphthalene (6.00 g, 37.9 mmol) in THF (60 mL) was added to a 200 mL flask equipped with a magnetic stirrer, an argon inlet, and a condenser. The solution was cooled to 0 °C, and then *n*-BuLi in hexane (47.4 mL, 75.8 mmol) was added dropwise. The reaction mixture was warmed up to room temperature and stirred additionally for 12 h. The resulting solution was cooled to 0 °C again, and then $ClSiMe_3$ (9.62 mL, 75.8 mmol) was added using a gas-tight syringe. The mixture was warmed up to room temperature and refluxed for 2 h. All volatiles were removed by drying in vacuo. The oily residue was extracted with pentane. After filtration, analytically pure dark purple oil (7.35 g, 64.0%) was obtained by evaporating the filtrate to dryness. ^1H NMR (C_6D_6): δ 7.32 (d, 2H), 7.22 (t, 2H), 6.71 (d, 2H), 5.41 (s, NH), 0.17 (s, 18H). ^{13}C NMR (C_6D_6): δ 145.3, 138.8, 126.7, 121.9, 116.8, 0.6. Anal. Calcd for $C_{16}H_{24}N_2Si_2$: C, 63.51; H, 8.66; N, 9.26. Found: C, 63.74; H, 8.77; N, 9.35.

Preparation of 1,8-$C_{10}H_6(NHSi(i\text{-}Pr)_3)_2$ (1b). The title compound was obtained by the same method as used for **1a** except using $ClSi(i\text{-}Pr)_3$ as the silylating reagent. Dark pink crystals were isolated from the recrystallization in pentane at −78 °C (yield = 72.4%). ^1H NMR (C_6D_6): δ 7.28 (d, 2H), 7.19 (t, 2H), 6.84 (d, 2H), 5.04 (s, NH), 1.32 (sept, 6H), 1.12 (d, 36H). ^{13}C NMR (C_6D_6): δ 145.4, 138.6, 126.2, 120.8, 114.2, 19.1, 13.6. Anal. Calcd for $C_{28}H_{50}N_2Si_2$: C, 71.42; H, 10.70; N, 5.95. Found: C, 71.72; H, 10.65; N, 5.91.

Preparation of 1,8-$C_{10}H_6(NLiSiMe_3)_2$ (2a). A hexane (30 mL) solution dissolving **1a** (5.30 g, 17.5 mmol) was cooled to −78 °C, and *n*-BuLi (22.0 mL, 35.2 mmol) was added slowly. As the reaction mixture was warmed up to room temperature, a yellow-brown precipitate began to be formed. After additional stirring for 3 or 4 h, the precipitate was isolated by filtration and washed with hexane three times. Drying in vacuo produced a yellow solid (4.70 g, 85.0%). ^1H NMR (THF-d_8): δ 6.72 (t, 2H), 6.50 (d, 2H), 6.25 (d, 2H), 0.20 (s, 18H). ^{13}C NMR (THF-d_8): δ 160.3, 140.9, 125.8, 114.2, 113.8, 2.78.

Preparation of 1,8-$C_{10}H_6(NLiSi(i\text{-}Pr)_3)_2$ (2b). A hexane (30 mL) solution dissolving **1b** (3.77 g, 8.00 mmol) was cooled to 0 °C, and *n*-BuLi (10.0 mL, 16.0 mmol) was added slowly. A yellow-green precipitate was formed immediately after the addition. The reaction mixture was stirred at room temperature for 12 h. After filtration and hexane washing, the precipitate was dried in vacuo to give a greenish yellow solid (3.00 g, 78.0%). ^1H NMR (C_6D_6): δ 7.28 (d, 4H), 6.81 (t, 2H), 1.24 (sept, 6H), 1.06 (d, 36H). ^{13}C NMR (C_6D_6): δ 155.4, 140.5, 126.6, 117.3, 116.8, 19.8, 14.7.

Preparation of {1,8-$C_{10}H_6(NSiMe_3)_2$}$TiCl_2$ (3a). The dilithiated compound **2a** (1.57 g, 5.00 mmol) in diethyl ether (50 mL) was added to $TiCl_4$ (5.00 mL, 5.00 mmol) solution dissolved in diethyl ether (20 mL) at 0 °C. The reaction mixture was warmed up to room temperature and stirred for 12 h. All volatiles were removed under vacuum, and the resulting residue was extracted with toluene and filtered through a Celite pad. Evaporating the filtrate in vacuo and subsequent washing with cold pentane gave a dark red-brown solid (1.12 g, 53.4%). An analytically pure microcrystal (24%) was obtained from the recrystallization in pentane at −78 °C. ^1H NMR (C_6D_6): δ 7.32 (d, 2H), 7.09 (t, 2H), 6.60 (d, 2H), 0.56 (s, 18H). ^{13}C NMR (C_6D_6): δ 148.5, 137.7, 126.7, 125.4, 1.88. Anal. Calcd for $C_{16}H_{24}N_2Si_2TiCl_2$: C, 45.82; H, 5.77; N, 6.68. Found: C, 46.16; H, 5.88; N, 6.85.

Preparation of {1,8-$C_{10}H_6(NSi(i\text{-}Pr)_3)_2$}$TiCl_2$ (3b). The dilithiated compound **2b** (1.00 g, 2.07 mmol) in diethyl ether (20 mL) was added to $TiCl_4$ (2.00 mL, 2.00 mmol) solution dissolved in ether (10 mL) at 0 °C. The reaction mixture was warmed up to room temperature and stirred for 12 h. All volatiles were removed under vacuum, and the resulting residue was extracted with hexane and filtered through a Celite pad. The volume of the filtrate was reduced to 15 mL, and the solution was stored at −20 °C for 12 h. Dark red crystals (300 mg, 24.3%) were isolated by filtration. ^1H NMR (C_6D_6): δ 7.24 (d, 2H), 7.08 (t, 2H), 6.89 (d, 2H), 1.61 (sept, 6H), 1.03 (d, 36H). ^{13}C NMR (C_6D_6): δ 147.2, 135.8, 126.2, 125.2, 118.5, 19.0, 14.8. Anal. Calcd for $C_{28}H_{48}N_2Si_2TiCl_2$: C, 57.22; H, 8.23; N, 4.77. Found: C, 57.15; H, 8.20; N, 4.44.

Preparation of {1,8-$C_{10}H_6(NSiMe_3)_2$}$_2$Zr (4a). The compound **2a** (628 mg, 2.00 mmol) in diethyl ether (20 mL) was added to $ZrCl_4$ (466 mg, 2.00 mmol) suspended in diethyl ether (15 mL) at 0 °C. The reaction mixture was warmed up to room temperature and stirred overnight. Solvent was removed under vacuum, and the resulting yellow-brown solid was extracted with pentane three times (3 × 25 mL) and filtered through a Celite pad to give a clear orange solution. The filtrate was concentrated to 25 mL and stored at −20 °C. Yellow microcrystals (250 mg, the yield based on the consumed $ZrCl_4$ is 40%) were isolated by filtration. The variable-temperature ^1H NMR (500 MHz) spectra of **4a** were recorded in toluene-d_8. 300 K: δ 7.22 (br d, 4H), 7.14 (br s, 4H), 6.60 (br s, 4H), 0.14 (br s, 36H). 343 K: δ 7.20 (d, 4H), 7.07 (t, 4H), 6.56 (d, 4H), 0.12 (s, 36H). 233 K: δ 7.35 (d, 2H), 7.26 (t, 2H), 7.18 (d, 2H), 7.02 (t, 2H), 6.91 (d, 2H), 6.44 (d, 2H), 0.38 (s, 18H), −0.01 (s, 18H). ^{13}C NMR (toluene-d_8, 300 K): δ 139.7, 137.5, 129.2, 127.0, 126.5, 1.83. Anal. Calcd for $C_{32}H_{48}N_4Si_4Zr$: C, 55.51; H,7.00; N, 8.09. Found: C, 55.72; H, 7.35; N, 8.16.

Preparation of {1,8-$C_{10}H_6(NSi(i\text{-}Pr)_3)_2$}$ZrCl_2$ (4b). To a 100 mL Schlenk flask charged with the compound **2b** (1.00 g, 2.07 mmol) and $ZrCl_4$ (480 mg, 2.07 mmol) was added diethyl ether (30 mL) precooled at 0 °C. As the reaction mixture was warmed up to room temperature, the color of the solution gradually changed to yellow-orange with the concurrent formation of a yellow-brown precipitate. The solution was stirred overnight. The solvent was removed under vacuum, the resulting orange solid was extracted with hexane, and subsequently the solution was filtered. The filtrate was concentrated and stored at −45 °C overnight. Orange crystals (600 mg, 46.2%) were isolated by filtration. ^1H NMR (C_6D_6): δ 7.22 (d, 2H), 7.07 (t, 2H), 6.95 (d, 2H), 1.46 (sept, 6H), 1.04 (d, 36H). ^{13}C NMR (C_6D_6): δ 143.2, 136.9, 126.4, 124.2, 121.7,

---

(5) Despite several trials for elemental analysis, the low carbon content was measured repeatedly.

19.2, 14.2. Anal. Calcd for $C_{28}H_{48}N_2Si_2ZrCl_2$: C, 53.30; H, 7.67; N, 4.43. Found: C, 52.92; H, 7.60; N, 4.42.

Reaction between 3a and AlMe$_3$. To a Teflon-valved NMR tube charged with compound **3a** (21 mg, 50 μmol) in C_6D_6 (0.8 mL) was added 2 equiv of $AlMe_3$ (10 μL, 104 μmol) at room temperature. NMR spectra were recorded to follow the reaction.

Reaction between 3b and AlMe$_3$. To a Teflon-valved NMR tube charged with **3b** (29 mg, 50 μmol) and C_6D_6 (0.8 mL) was added slowly 2 equiv of $AlMe_3$ (10 μL, 104 μmol) at room temperature. NMR spectra were recorded to follow the reaction.

Preparative Scale. A solution of **3b** (0.29 g, 0.49 mmol) and $AlMe_3$ (200 μL, 2.09 mmol) in toluene (20 mL) was stirred at room temperature for 1 h. The solution was heated up to 60 °C and stirred additionally at this temperature for 3 h. Toluene and unreacted $AlMe_3$ were removed in vacuo, the resulting deep red solid was extracted with pentane, and the solution was filtered. The filtrate was concentrated and cooled to −45 °C overnight. Deep red crystals (220 mg, 80%) were isolated by filtration, washed with cold pentane, and dried under vacuum. ^{1}H NMR: δ 7.26 (d, 2H), 7.13 (t, 2H), 6.89 (d, 2H), 1.67 (sept, 6H), 1.48 (s, 3H), 1.11 (d, 18H), 1.05 (d, 18H). ^{13}C NMR: δ 147.7, 136.8, 126.3, 124.1, 117.4, 63.3, 19.5, 19.2, 14.7. Anal. Calcd for $C_{29}H_{51}N_2Si_2TiCl$: C, 61.40; H, 9.06; N, 4.94. Found: C, 61.66; H, 8.71; N, 5.04.

Reaction between 4b and AlMe$_3$. To a Teflon-valved NMR tube charged with **4b** in C_6D_6 was added slowly excess $AlMe_3$ at room temperature. NMR spectra were recorded to follow the reaction.

Preparation of the Dinuclear Aluminum Complex (5) from 1a and Trimethylaluminum. The trimethylaluminum (1.50 mL, 15.6 mmol) solution in hexane (30 mL) was added slowly to a **1a** (2.00 g, 6.61 mmol) solution in hexane at 0 °C. As the reaction mixture was warmed slowly up to room temperature, white precipitate was formed gradually. After additional stirring overnight, the solution was filtered, and the residual precipitate was extracted with hexane. The combined hexane solution was concentrated and stored at −20 °C overnight. White crystalline **5** (1.05 g) was isolated by filtration. The precipitate remaining from the previous filtration was dissolved in toluene, and the toluene filtrate was concentrated and recrystallized at −20 °C to give a second crop (0.915 g) of the product **5**. The combined yield of the two crops was 72%. ^{1}H NMR: δ 7.28 (d, 2H), 7.06 (m, 4H), 0.40 (s, 18H), −0.11 (s, 6H), −1.14 (s, 6H). ^{13}C NMR: δ 145.0, 136.3, 125.5, 124.2, 118.2, 110.8, 2.11, −0.48, −8.21. Anal. Calcd for $C_{20}H_{36}N_2Si_2Al_2$: C, 57.93; H, 8.75; N, 6.76. Found: C, 56.75; H, 8.94; N, 6.68.[5]

Reaction of 3a,b with MAO. To a Teflon-valved NMR tube charged with each diamido complex (20 μmol) and MAO (200 or 400 μmol) was added toluene-d_8 (1.0 mL) at room temperature. ^{1}H NMR spectra were recorded to follow reactions of each solution.

Polymerization of Ethylene. In a glovebox a 100 mL Schlenk tube was charged with a catalyst together with MAO and toluene. The mixture was stirred at room temperature for 10 min. Ethylene gas was then allowed into the tube, and its pressure was maintained continuously at 1 atm by means of a mercury bubbler. The polymerization was quenched by stopping the ethylene supply and subsequent addition of a methanolic solution of 1 M HCl. The white precipitate was filtered off, washed with an aqueous solution of 1 M HCl and copious methanol and acetone, and finally dried in an oven at 80 °C for 12 h.

X-ray Crystallographic Determination for 3a,b, 4a, and 5. Crystals of each complex were obtained by recrystallization from hexane or pentane. Each crystal sealed in a capillary tube was mounted on an Enraf-Nonius CAD4 diffractometer using graphite-monochromated Mo Kα (λ = 0.710 73 Å) radiation. Unit cell parameters were determined by least-squares refinement of 25 reflections. Data collection was performed at 293 K. The intensity data were corrected for Lorentz and polarization effects. The structures were solved by direct methods (SHELXS-86) and refined by full-matrix least-squares methods (SHELXL-93). All non-hydrogen atoms were refined anisotropically, and their positions were calculated (C−H = 0.95 Å) and included in the final cycles of refinement.

X-ray Crystallographic Determination for 4b. An orange crystal was mounted on a Siemens SMART diffractometer equipped with a graphite-monochromated Mo Kα (λ = 0.710 73 Å) radiation source and a CCD detector. Fifteen frames of two-dimensional diffraction images were collected and were processed to deduce a cell parameter and orientation matrix. Data collection was performed at 293 K. A total of 1271 frames of two-dimensional diffraction images were collected, each of which was measured for 20 s. The frame data were processed to produce conventional intensity data by the program SAINT. The intensity data were corrected for Lorentz and polarization effects. An absorption correction was also applied based on ψ scans. The structure was solved by a combination of Patterson and difference Fourier methods provided by the program package SHELXTL. All of the non-hydrogen atoms were refined anisotropically.

Results and Discussion

Preparation of N,N′-Disilylated 1,8-Diaminonaphthalene. Commercially available 1,8-diaminonaphthalene can be regioselectively silylated to give N,N′-disilylated products (eq 1). The silylation with trimethylchlorosilane and tris(isopropyl)chlorosilane gives a dark purple oil (**1a**) and dark pink crystals (**1b**), respectively, in moderate yields using an analogous method reported previously.[3d,6]

$$1,8\text{-}C_{10}H_6(NH_2)_2 \xrightarrow[\text{2) 2 RCl}]{\text{1) 2 }^{n}\text{BuLi}} \underset{\mathbf{1a,b}}{1,8\text{-}C_{10}H_6(NHR)_2} \tag{1}$$

1a R = $SiMe_3$
1b R = $Si(i\text{-}Pr)_3$

Preparation of the Diamido Group 4 Metal Complexes. The silylated products were lithiated with 2 equiv of *n*-BuLi in hexane. Filtration and washing with copious hexane produced yellow solids (eq 2). When the dilithiated solid (**2a**) was allowed to react with an equimolar amount of titanium tetrachloride, an expected product, a mono(diamido)titanium dichloride (**3a**), was obtained as the sole product, but the isolated yield of the complex was low due to its high solubility in hydrocarbon solvents. In contrast, the reaction with zirconium tetrachloride produced a bis(diamido)zirconium(IV) complex (**4a**). In contrast, the bulkier dilithiated solid (**2b**) gave mono(diamido) complexes (**3b**, **4b**) in both cases. The difference must result from the relative size of the metal ions and the relative steric demand of the diamido ligands, as can be similarly found in syntheses of related group 4 metal diamido complexes.[3a,6,7]

---

(6) Aoyagi, K.; Gantzel, P. K.; Kalai, K.; Tilley, T. D. *Organometallics* **1996**, *15*, 923.

(7) (a) Horton, A. D.; de With, J. *Organometallics* **1997**, *16*, 5424. (b) Tsuie, B,; Swenson, D. C.; Jordan, R. F. *Organometallics* **1997**, *16*, 1392. (c) Bürger, H.; Geschwandner, W.; Liewald, G. R. *J. Organomet. Chem.* **1983**, *259*, 145. (d) Brauer, D. J.; Bürger, H.; Essig, E.; Geschwandner, W. *J. Organomet. Chem.* **1980**, *190*, 343.

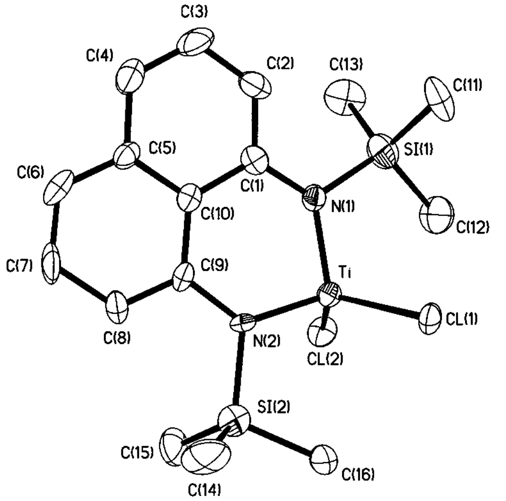

Figure 1. ORTEP diagram of $\{1,8\text{-}C_{10}H_6(NSiMe_3)_2\}TiCl_2$ (**3a**).

In order to prepare alkyl derivatives of the mono(diamido) complexes, reactions of **3a**, **3b**, and **4b** with methyllithium and several Grignard reagents (MeMgCl, MeMgBr, and $PhCH_2MgCl$) were carried out, but only unidentified materials were obtained.

$$\underset{\textbf{1a,b}}{1,8\text{-}C_{10}H_6(NHR)_2} \xrightarrow[\text{hexane}]{2\ ^{n}BuLi} \underset{\textbf{2a,b}}{1,8\text{-}C_{10}H_6(NRLi)_2} \qquad (2)$$

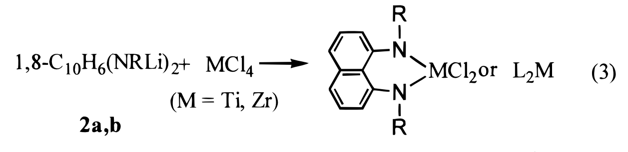

3a M = Ti, R = $SiMe_3$
3b M = Ti, R = Si(*i*-Pr)$_3$
4a M = Zr, R = $SiMe_3$
4b M = Zr, R = Si(*i*-Pr)$_3$

Characterization of $\{1,8\text{-}C_{10}H_6(NSiMe_3)_2\}TiCl_2$ (3a) and $\{1,8\text{-}C_{10}H_6(NSi(i\text{-}Pr)_3)_2\}TiCl_2$ (3b). The title titanium(IV) complexes have been characterized by NMR spectroscopy and elemental analysis. A sharp resonance of the methyl protons in ^1H NMR spectra shows that the rotation of the methyl group around the silicon−nitrogen bond is fast. Also, the symmetric splitting pattern of the aromatic ring shows that the chemical environments of both sides of the ring are equivalent. The symmetric environment of **3a** in solution is also maintained in the solid state to a certain degree, but such is not the case for **3b** (vide infra).

The molecular structure of **3a** is shown in Figure 1. Selected bond lengths and angles of **3a** are summarized in Table 1. Compound **3a** has an approximately 2-fold axis which passes through the Ti atom and C(10) and C(5) atoms of the naphthalene ring and, consequently, has C_2 symmetry. A six-membered chelate ring consisting of Ti, N(1), C(1), C(10), C(9), and N(2) atoms is nearly planar. The Si(1), N(1), Ti, N(2), and Si(2) atoms lie on a plane, and the plane defined by these atoms is about 8.6° from being coplanar with the naphthalene plane. The geometry around the titanium atom is distorted tetrahedral. As in other reported titanium diamido complexes,[3f,g,6,7b] a small N(1)−Ti−N(2) bite angle (97.0°) and large Cl(1)−Ti−Cl(2) opposite angle (120.5°) relative to titanocene complex (130.89° and 94.43°, respectively)[8] are observed for **3a**. In comparison, the bite angle of the naphthalene diamide ligand is similar to that (99.2°) of the propylene diamide ligand of the McConville catalyst, $[ArN(CH_2)_3NAr]TiCl_2$ (Ar = 2,6-*i*-$Pr_2C_6H_3$).[3f] Interestingly, the Cl−Ti−Cl angle of **3a** is larger than those of the previously reported titanium diamido complexes (McConville catalyst, 107.77°; $[1,2\text{-}C_6H_4(NSi(i\text{-}Pr)_3)_2]TiCl_2$,[6] 109.6°; $[1,2\text{-}C_2H_4\text{-}(NSiMe_3)_2]TiCl_2$,[3h] 110.73°; $[1,2\text{-}(NSiMe_3)_2C_6H_{10}]TiI_2$,[7b] 115.45°), which is presumably due to the significant constraint on the symmetrically crowded geometry provided by the extremely rigid naphthalene link of **3a**. As in a space-filling view (not shown), the spaces above and below the Cl(1)−Ti−Cl(2) plane are adjustably surrounded by the methyl groups of *N*-silyl substituents. Consequently, the chloride atoms in the coordination wedge strongly feel the presence of methyl hydrogens of the $SiMe_3$ substituents (Cl(1)···C(16) = 3.327(17) Å, Cl(2)···C(12) = 3.338(21) Å). This may lead to an unusually large Cl(1)−Ti−Cl(2) angle. The Ti−N (1.862, 1.873 Å) and Ti−Cl (2.255, 2.271 Å) bond lengths are comparable to those in the titanium(IV) diamido complexes mentioned above. Both amides are sp^2-hydridized as evidenced by the sum of the angles about each nitrogen (N(1) = 360.0°, N(2) = 359.7°), and it can be assumed that each nitrogen atom donates four electrons to the electrophilic titanium center.

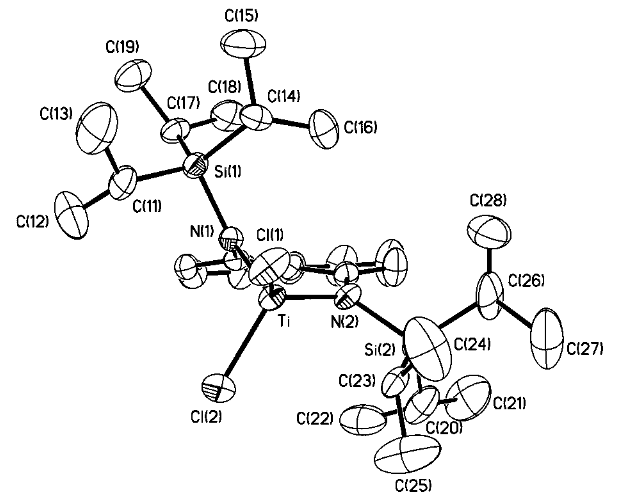

Figure 2. ORTEP diagram of $\{1,8\text{-}C_{10}H_6(NSi(i\text{-}Pr)_3)_2\}\text{-}TiCl_2$ (**3b**).

Table 1. Selected Bond Distances (Å) and Bond Angles (deg) for $\{1,8\text{-}C_{10}H_6(NSiMe_3)_2\}TiCl_2$ (3a)

Ti−N(1)	1.862(11)	Ti−N(2)	1.873(12)
Ti−Cl(1)	2.255(5)	Ti−Cl(2)	2.271(5)
Si(1)−N(1)	1.800(12)	Si(2)−N(2)	1.795(10)
N(1)−C(1)	1.43(2)	N(2)−C(9)	1.42(2)
N(1)−Ti−N(2)	97.0(5)	N(1)−Ti−Cl(2)	111.6(4)
N(2)−Ti−Cl(2)	105.7(4)	Cl(1)−Ti−Cl(2)	120.5(2)
C(1)−N(1)−Si(1)	120.3(9)	Ti−N(1)−C(1)	126.9(10)
Ti−N(1)−Si(1)	112.8(6)		

The molecular structure of **3b** is shown in Figure 2. Selected bond lengths and angles of **3b** are summarized

---

(8) Clearfield, A.; Warner, D. K.; Saldarriga-Molina, C. H.; Ropal, R. I. *Can. J. Chem.* **1975**, *53*, 1622.

Table 2. Selected Bond Distances (Å) and Bond Angles (deg) for $\{1,8\text{-}C_{10}H_6(NSi(i\text{-}Pr)_3)_2\}TiCl_2$ (3b)

Ti–N(1)	1.838(6)	Ti–N(2)	1.881(6)
Ti–Cl(1)	2.235(3)	Ti–Cl(2)	2.239(3)
Si(1)–N(1)	1.804(6)	Si(2)–N(2)	1.805(6)
N(1)–C(1)	1.442(8)	N(2)–C(9)	1.433(9)
Ti–C(1)	2.636(7)		
N(1)–Ti–N(2)	99.1(3)	N(1)–Ti–Cl(1)	107.8(2)
N(2)–Ti–Cl(1)	119.4(2)	N(1)–Ti–Cl(2)	107.1(2)
N(2)–Ti–Cl(2)	113.7(2)	Cl(1)–Ti–Cl(2)	108.48(11)
C(1)–N(1)–Si(1)	122.0(5)	Ti–N(1)–C(1)	106.4(4)
Ti–N(1)–Si(1)	131.4(3)	C(9)–N(2)–Si(2)	116.5(5)
Ti–N(2)–C(9)	118.9(5)	Ti–N(2)–Si(2)	122.2(3)

in Table 2. Unlike complex **3a**, a six-membered chelate ring is highly puckered, and the titanium atom does not lie in the naphthalene plane. The *N*-silyl groups are in an asymmetrical environment, where one silyl group is positioned significantly away from the naphthalene plane and the other nearly along with the plane. The geometry around the titanium atom is distorted tetrahedral. A small N(1)–Ti–N(2) angle (99.1°) and a large Cl(1)–Ti–Cl(2) angle (108.48°) are also observed for **3b**. The latter angle is close to the value (107.77°) found in the titanium complex reported by McConville and coworkers.[3f] The present Ti–N(1) (1.838 Å) and Ti–N(2) (1.881 Å) lengths are slightly different from each other, whereas the Ti–Cl(1) (2.235 Å) and Ti–Cl(2) (2.239 Å) lengths are in the normal range. In contrast to **3a**, it seems that there is an interaction between the titanium atom and the naphthalene ring (Ti–C(1) = 2.636 Å). This interaction is much weaker than that found previously in a diamido complex such as $[1,2\text{-}C_6H_4(NSi(i\text{-}Pr)_3)_2]TiCl_2$ (Ti–C_{ipso} = 2.349, 2.353 Å).[6] In spite of the highly asymmetric environment of *N*-silyl groups, each nitrogen atom is also nearly sp^2-hybridized (sum of angles around N(1) = 359.8°, N(2) = 357.6°).

Characterization of $\{1,8\text{-}C_{10}H_6(NSiMe_3)_2\}_2Zr$ (4a) and $\{1,8\text{-}C_{10}H_6(NSi(i\text{-}Pr)_3)_2\}ZrCl_2$ (4b). The title zirconium(IV) complexes have been characterized by NMR spectroscopy and elemental analysis. It is found that the less sterically demanding ligand coordinates the zirconium center to form a bis(diamido) complex (**4a**). Contrastingly, a mono(diamido)zirconium(IV) complex (**4b**) was formed with the bulkier ligand. Broad resonances for **4a** at room temperature in ^{1}H NMR contrast with the sharp ones for **4b**. As suggested in the crystal structure of **4a** (Figure 3), there are two sets of resonances in the ^{1}H NMR spectrum. For example, both sites of the two trimethylsilyl groups attached to the N(1) and N(4) atoms are equivalent. By the same token, the two trimethylsilyl groups on the N(2) and N(3) atoms are equivalent. It is observed that these two sets of trimethylsilyl groups resonate at different frequencies at room temperature. This ^{1}H NMR observation shows that the molecular structure in the solid state is maintained in solution.

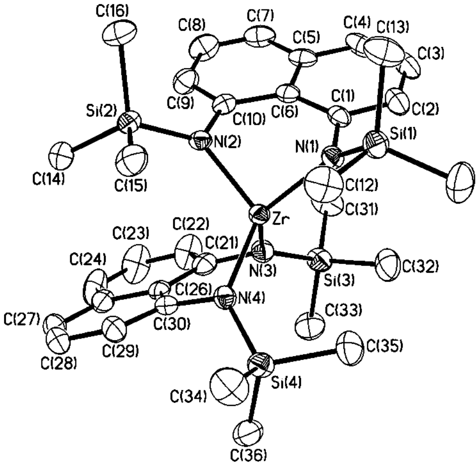

Figure 3. ORTEP diagram of $\{1,8\text{-}C_{10}H_6(NSiMe_3)_2\}_2Zr$ (**4a**).

Table 3. Selected Bond Distances (Å) and Bond Angles (deg) for $\{1,8\text{-}C_{10}H_6(NSiMe_3)_2\}_2Zr$ (4a)

Zr–N(1)	2.053(3)	Zr–N(2)	2.040(3)
Zr–N(3)	2.048(4)	Zr–N(4)	2.047(4)
Zr–C(1)	2.802(4)	Zr–C(10)	2.772(4)
Zr–C(21)	2.801(5)	Zr–C(30)	2.791(5)
N(1)–C(1)	1.425(6)	N(2)–C(10)	1.406(5)
N(3)–C(21)	1.413(6)	N(4)–C(30)	1.430(6)
N(1)–Zr–N(2)	90.67(14)	N(3)–Zr–N(4)	90.3(2)
N(2)–Zr–N(3)	109.1(2)	N(2)–Zr–N(4)	117.26(14)
N(1)–Zr–N(3)	118.4(2)	N(1)–Zr–N(4)	131.5(2)
Zr–N(1)–C(1)	105.9(3)	Zr–N(1)–Si(1)	131.6(2)
Zr–N(2)–C(10)	105.6(3)	Zr–N(2)–Si(2)	131.5(2)
Zr–N(3)–C(21)	106.6(3)	Zr–N(3)–Si(3)	130.6(2)
Zr–N(4)–C(30)	105.4(3)	Zr–N(4)–Si(4)	132.9(2)

In order to unveil exchange processes in **4a**, variable-temperature ^{1}H NMR (500 MHz) experiments were carried out. Heating toluene solutions of **4a** enhances the exchange rate, in turn giving sharp resonances. On cooling to 280 K the resonances coalesce to give a broad peak. Further cooling to 233 K yields two sharp resonances representing two nonequivalent trimethylsilyl groups. The free energy of the rotational barrier, $\Delta G^\ddagger$, is calculated to be 13 kcal mol^{-1} from the coalescence temperature in the ^{1}H NMR spectrum.

In the molecular structure of **4a**, two naphthalene diamido ligands are related each other by a 2-fold axis which passes through the zirconium atom and bisects the N(1)–Zr–N(4) angle. The six-membered chelate rings are not planar, and they fold along the N–N axis by about 60°. The Zr–C_{ipso} interatomic distances (average 2.79 Å) are too long for the Zr–aromatic ring interaction, and no evidence of the interaction in solution is observed in the ^{13}C NMR spectrum. The geometry around the zirconium atom is highly distorted tetrahedral so that the N–Zr–N angles (average 90.5°) of the six-membered chelate rings are much smaller than that of an ideal tetrahedron (Table 3). Meanwhile, the Zr–N bond distances (average 2.05 Å) are comparable to those of other related zirconium(IV) diamido complexes.[3d] Each nitrogen atom is in an sp^2-hybridized environment, as indicated by the sum of the angles around the nitrogen. These structural features of **4a** are quite similar to those of the bis(diamido)zirconium(IV) complex, $[1,2\text{-}C_6H_4(NSi(i\text{-}Pr)_3)_2]_2Zr$, having a phenylene linker, although the latter complex has somewhat smaller N–Zr–N angles (average 86.3°) and shorter Zr–C_{ipso} bond distances (average 2.60 Å).[6]

The mono(diamido) complex **4b** (Figure 4) exists as a dimer connected through two chloride bridges in the solid state,[9] and two molecular units comprising the dimer are each constrained by a crystallographic center of inversion. An electrophilic zirconium atom is additionally stabilized by partial π donation of a chloride ligand of the other metallic center. Bond distances

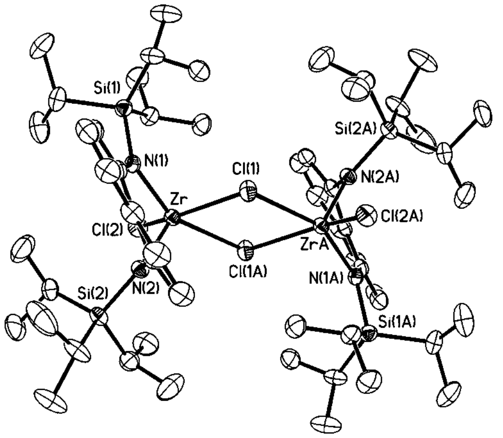

Figure 4. ORTEP diagram of the {1,8-$C_{10}H_6(NSi(i\text{-}Pr)_3)_2$}-$ZrCl_2$ dimer (**4b**).

Table 4. Selected Bond Distances (Å) and Bond Angles (deg) for the {1,8-$C_{10}H_6(NSi(i\text{-}Pr)_3)_2$}$ZrCl_2$ Dimer (4b)[a]

Zr−N(1)	2.071(3)	Zr−N(2)	1.974(3)
Zr−Cl(2)	2.3911(13)	Zr−Cl(1)	2.610(2)
Zr−Cl(1A)	2.6817(14)	Zr−C(9)	2.685(4)
Si(1)−N(1)	1.785(3)	Si(2)−N(2)	1.803(3)
N(1)−C(1)	1.429(5)	N(2)−C(9)	1.455(5)
N(1)−Zr−N(2)	94.17(13)	N(1)−Zr−Cl(2)	104.95(9)
N(2)−Zr−Cl(2)	99.56(9)	N(1)−Zr−Cl(1)	89.50(9)
N(2)−Zr−Cl(1)	108.03(9)	Cl(2)−Zr−Cl(1)	147.83(4)
N(1)−Zr−Cl(1A)	153.81(9)	N(2)−Zr−Cl(1A)	109.38(10)
Cl(2)−Zr−Cl(1A)	82.84(5)	Cl(1)−Zr−Cl(1A)	72.75(5)
Zr−Cl(1)−Zr(A)	107.25(5)	C(1)−N(1)−Si(1)	119.5(3)
Zr−N(1)−C(1)	116.1(2)	Zr−N(1)−Si(1)	123.6(2)
C(9)−N(2)−Si(2)	119.1(2)	Zr−N(2)−C(9)	102.0(2)
Zr−N(2)−Si(2)	138.3(2)		

[a] Symmetry transformations used to generate equivalent atoms: A, $-x$, $-y + 1$, $-z + 1$.

(2.682, 2.610 Å) from each zirconium atom to the nonequivalent bridging chloride ligands are elongated from the Zr−$Cl_{terminal}$ distance (2.391 Å), and Zr···Zr separation is 4.261(2) Å (Table 4). The Zr−$Cl_{bridging}$−Zr and $Cl_{bridging}$−Zr−$Cl_{bridging}$ angles are 107.25° and 72.75°, respectively. Therefore, the two zirconium centers and two chlorides are coplanar. The geometry about each zirconium atom can be described as distorted square pyramidal, in which the N(2) atom and the remaining four atoms (N(1), Cl(2), Cl(1), Cl(1A)) are in axial and basal (about 0.04 Å deviation from planarity) positions, respectively. As in the case of **3b**, the interaction (2.69 Å) between the zirconium atom and one ipso carbon of naphthalene is weak. The interaction not only breaks the planarity of the six-membered chelate ring but also generates asymmetry in terms of the Zr−amide bond distance (2.071 Å vs 1.974 Å). The N(1)−Zr−N(2) chelate angle (94.17°) is somewhat more acute than that of **3b**. The dihedral angle between the planes containing Si(1), N(1), Zr and Zr, N(2), Si(2) is about 71.2°, reflecting the fact that one Si group is farther away from the naphthalene plane. These structural differences between complexes **3b** and **4b** can be attributed to the larger size of the zirconium(IV) center relative to the titanium(IV) center. Also, each nitrogen atom is in an sp^2-hybridized environment, as indicated by the sum of the angles around the nitrogens.

Reaction between 3a and $AlMe_3$. Immediately after the mixing of **3a** with 2 equiv of trimethylaluminum at room temperature, new ^1H resonance signals are recorded in the NMR spectrum: δ 7.30 (d, 2H), 7.11 (t, 2H), 6.69 (d, 2H), 1.17 (s, TiMe), 0.44 (s, 18H). A resonance (δ 1.17 ppm) in the ^1H NMR spectra is indicative of the monomethylated product, {[1,8-$C_{10}H_6(NSiMe_3)_2$]Ti(Me)Cl}. In 5 min, 60% of **3a** was converted to the monomethyl complex. At the same time, new resonances also appear, which are assigned to those of a dinuclear aluminum compound {[1,8-$C_{10}H_6(NSiMe_3)_2$]-$(AlMe_2)_2$}. This aluminum compound can be synthesized from an independent reaction between 1,8-$C_{10}H_6(NHSiMe_3)_2$ and $AlMe_3$ (vide infra). While most of the unreacted $AlMe_3$ disappears in 24 h, the expected dimethyl titanium complex is not observed. Whereas the total amount of **3a** and monomethyl complex relative to that in the beginning of the reaction decreased to some extent, the amount of dinuclear aluminum compound increased only slightly (10%). When the solution was heated at 55 °C for 1 h, the amount of the latter aluminum compound relative to the monomethyl complex increased to a certain degree. Heating at 55 °C for several hours produced the aluminum compound exclusively (25% NMR yield based on the amount of added **3a**) with concurrent formation of a black precipitate. Therefore, the transmetalation of mono(diamido)titanium(IV) complex occurred to form an aluminum complex under these particular reaction conditions. Similar transmetalation has recently been proposed by Jordan and co-workers in a reaction of L_2MX_2 (M = Zr, L = 2-Me-5,7-Br_2-8-quinolinolato, X = Cl; M = Ti or Zr, L = 2-pyridyl-1,1′-bisalkylmethanolato or 2-pyridyl-1,1′-bisarylmethanolato, X = CH_2Ph, NMe_2) with $AlMe_3$.[10] Therefore, it is believed that the transmetalation is a rather general type of reaction for diamido metal complexes.

Reaction between 3b and $AlMe_3$. With 2 equiv of trimethylaluminum, conversion of **3b** to the monomethyl titanium complex {[1,8-$C_{10}H_6(NSi(i\text{-}Pr_3)_2$]Ti(Me)Cl} was observed. In 5 min, the conversion was 85% (based on NMR analysis). Longer reaction times do not improve the conversion yield. When the solution was heated at 55 °C for 1 h, the conversion percentage did not changed. In contrast to **3a**, the color of the solution remains dark red, and formation of a dinuclear aluminum compound or black precipitate was not observed under these reaction conditions.

Reaction between 4b and $AlMe_3$. The methylation of **4b** was not observed at all at room temperature. Neither the methylated product nor decomposition of starting complexes was observed when the mixture was heated at a higher temperature such as 55 °C for several hours.

Reaction of 1a with Trimethylaluminum. The bis(trimethylsilyl) diamido ligand (**1a**) reacts with 2 equiv of trimethylaluminum with concurrent formation

---

(9) For examples of zirconium(IV) diamido dichlorides with a dimeric structure: (a) Schattermann, F.; Schrock, R. R.; Davis, W. M. *Organometallics* **1998**, *17*, 989. (b) Cloke, F. G. N.; Hitchcock, P. B.; Love, J. B. *J. Chem. Soc., Dalton Trans.* **1995**, 25. (c) Polamo, M.; Leskelä, M. *J. Chem. Soc., Dalton Trans.* **1996**, 4345.

(10) (a) Bei, X.; Swenson, D. C.; Jordan, R. F. *Organometallics* **1997**, *16*, 3282. (b) Tsukahara, T.; Swenson, D. C.; Jordan, R. F. *Organometallics* **1997**, *16*, 3303. (c) Kim, I.; Nishihara, Y.; Jordan, R. F. *Organometallics* **1997**, *16*, 3314.

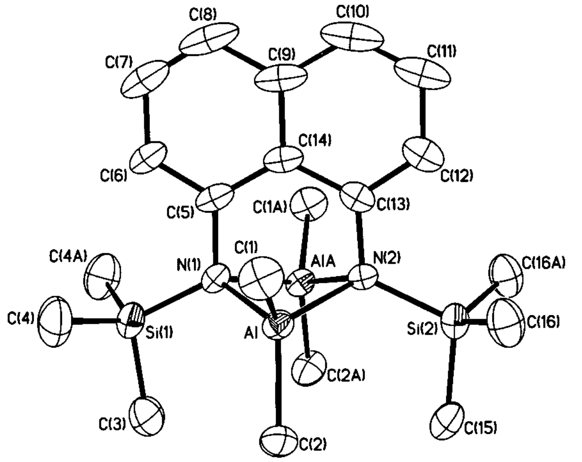

Figure 5. ORTEP diagram of $\{1,8\text{-}C_{10}H_6(NSiMe_3)_2\}Al_2Me_4$ **(5)**.

of methane at room temperature in 72% yield (eq 4). A white precipitate of the product can be easily obtained from hexane solution.

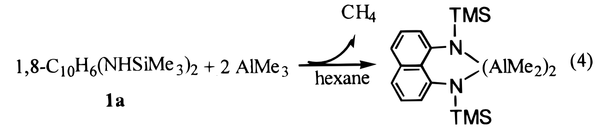

1a **5**

Characterization of $\{1,8\text{-}C_{10}H_6(NSiMe_3)_2\}Al_2Me_4$ (5). The title dinuclear aluminum complex has been characterized by NMR spectroscopy and elemental analysis. ^1H NMR spectroscopy shows that there are two different types of methyl groups, and each peak corresponds to six protons. The analysis suggests that the ligand coordinates two aluminum centers, and each center has two intact methyl groups.

The molecular structure of **5** is shown in Figure 5. Indeed, the product contains two aluminum centers, and the four methyl groups are positioned in two different chemical environments. Dinuclear complex **5** has a perfect C_{2v} symmetry, i.e., there is a mirror plane passing through Si(1), N(1), N(2), and Si(2) atoms, and another one passing through two aluminum atoms while being perpendicular to the former one. The geometry of each aluminum atom and nitrogen atom is distorted tetrahedral. The two nitrogen centers and two aluminum centers comprise a metallacycle in a butterfly shape. Each aluminum center is 1.42 Å away from a mirror plane bisecting the aluminum centers, and the angle between two AlN_2 planes is 143.7°. The formation of the puckered Al_2N_2 ring is mainly a consequence of the rigid naphthalene link. Complex **5** is structurally similar to a recently reported dinuclear aluminum complex, $\{(t\text{-}BuNCH_2CH_2N\,t\text{-}Bu)(AlH_2)_2\}$,[11] in which two AlH_2 moieties are symmetrically chelated by a N,N′-di-*tert*-butylethylenediamine ligand. As a result of the puckered Al_2N_2 ring, the N(1)−Al−N(2) angle (83.0°) of **5** is more acute than the Al−N(1)−Al(A) bond angle (90.7°) (Table 5). However, the Al−N bond distances (average 2.00 Å) are comparable to those of other dimeric aluminum amido complexes having a four-membered planar Al_2N_2 ring.[12]

Table 5. Selected Bond Distances (Å) and Bond Angles (deg) for $\{1,8\text{-}C_{10}H_6(NSiMe_3)_2\}(AlMe_2)_2$ (5)[a]

Al−N(1)	1.998(4)	Al−N(2)	1.995(4)
Al−C(1)	1.937(6)	Al−C(2)	1.949(5)
Si(1)−N(1)	1.779(6)	Si(2)−N(2)	1.804(6)
N(1)−C(5)	1.473(9)	N(2)−C(13)	1.441(9)
Al−Al(A)	2.842(3)		
N(1)−Al−N(2)	83.0(2)	N(1)−Al−C(1)	114.7(2)
N(1)−Al−C(2)	115.8(3)	N(2)−Al−C(1)	114.2(3)
N(2)−Al−C(2)	115.5(2)	C(1)−Al−C(2)	111.1(3)
Al−N(1)−Si(1)	119.7(2)	Al−N(1)−Al(A)	90.7(2)
C(5)−N(1)−Al(A)	101.8(3)	Al−N(1)−C(5)	101.8(3)
Si(1)−N(1)−Al(A)	119.7(2)	C(5)−N(1)−Si(1)	118.3(5)

[a] Symmetry transformations used to generate equivalent atoms: A, −*x*, *y*, *z*.

Reaction of 1b with Trimethylaluminum. A mixture of the diamine ligand **1b** and $AlMe_3$ was heated in toluene at 60 °C for 2 h in order to determine whether an aluminum complex can be prepared. However, only intact **1b** was recovered from the solution. This presumably results from significant steric hindrance of the bulky substituents on the nitrogen atoms. This observation explains the reason why the transmetalation was not observed during the heating of **3b** with trimethylaluminum.

Reaction of 3a,b with MAO. The reactions of **3a** and **3b** with a modified methylalumoxane (MAO) were followed by ^1H NMR spectroscopy. We employed MAO (from Akzo Co.) which is modified with isobutyl groups for enhanced solubility and shelf life. When **3a** was mixed with MAO (Al/Ti = 10) in toluene-d_8 at room temperature, the solution turned slowly to a dark red color with concurrent formation of insoluble deep purple material. Distinct new resonances appeared in the ^1H NMR spectrum as the major product and were assignable to a monoisobutyl titanium diamido complex ($Ti-CH_2CHMe_2$, 2.20 ppm; $-CH_2CHMe_2$, 1.80 ppm; $-CH_2CHMe_2$, 0.82 ppm). Also, the monomethyl titanium complex was observed as a minor product. The ratio of both monoalkylated products is 84:16. The formation of the monoisobutyl titanium complex as the sole product was confirmed from an independent reaction between **3a** and excess Al(*i*-Bu)$_3$, in which the reaction is complete (90%) in several minutes at room temperature.[13] At an Al:Ti ratio of 20, the formation of insoluble materials was so rapid that it was completed in several minutes. Only an isobutylated titanium complex was observed for this case. Unlike the reaction with $AlMe_3$, the transmetalated product **5** was not observed under these particular conditions. Because **5** was only observed after heating of the reaction mixture, it can be said that formation not of **5** but of an insoluble precipitate is the major deactivation process during the polymerization.

In contrast, mixing **3b** with MAO (Al:Ti = 10 or 20) did not produce the insoluble precipitate. Immediately after mixing, formation of the monomethyl titanium

---

[11] Atwood, J. L.; Lawrence, S. M.; Raston, C. L. *J. Chem. Soc., Chem. Commun.* **1994**, 73.

[12] (a) Byers, J. J.; Pennington, W. T.; Robinson, G. H.; Hrncir, D. C. *Polyhedron* **1990**, *9*, 2205. (b) Hess, H.; Hinderer, A.; Steinhauser, S. *Z. Anorg. Allg. Chem.* **1970**, *377*, 1.

[13] ^1H NMR data for $[1,8\text{-}C_{10}H_6(NSiMe_3)_2]Ti(CH_2CHMe_2)Cl$ (toluene-d_8): δ 7.23 (d, 2H), 7.14 (t, 2H), 6.69 (d, 2H), 2.19 (m, $Ti-CH_2CHMe_2$), 1.80 (d, $Ti-CH_2CHMe_2$), 0.82 (d, $Ti-CH_2CHMe_2$), 0.37 (s, 18H).

Table 6. Data for Ethylene Polymerization[a]

entry	catalyst	[cat.] (μmol)	time (min)	act.[b]	M_w[c]	M_n	PDI	T_m (°C)[e]
1	**3a**	10	10	12	insoluble			130.4
2	**3a**	10	30	20	insoluble			131.6
3	**3a**[f]	10	15	41	insoluble			131.4
4	**3a**[g]	5	15	66	62 418[d]	22 038	2.83	131.5
5	**3b**	10	30	12.6	5087	3625	1.40	129.8
6	**4b**	10	30	inactive				
7	Cp_2TiCl_2	20	10	350	573 000	215 090	2.66	138.1

[a] MMAO-4 (Al:M = 500), 50 mL of toluene, room temperature, 1 atm of ethylene. [b] kg PE/mol$_{cat}$ h atm. [c] Measured by GPC as calibrated with polystyrene standard; column temperature = 140 °C; elution solvent = 1,2,4-trichlorobenzene. [d] Partially soluble. [e] Measured by differential scanning calorimetry (DSC). [f] Al:Ti ~ 1000. [g] Al:Ti ~ 1000, 60−65 °C.

complex (Ti−*Me*, 1.42 ppm) and the monoisobutyl titanium complex (Ti−$CH_2C\mathit{H}Me_2$, 2.45 ppm; −$C\mathit{H}_2$-$CHMe_2$, 1.93 ppm; −$CH_2CH\mathit{Me}_2$, 0.89 ppm) as the major products was observed. The ratio of methylated to isobutylated product is 73:27 for Al:Ti = 10. Higher proportions of the isobutylated product (58%) are observed for Al:Ti = 20. The formation of the monoisobutyl titanium complex could be confirmed also from an independent reaction between **3b** and Al(*i*-Bu)$_3$.[14] The toluene solution retained a clear red color without any insoluble precipitates for as long as 1 h.

Polymerization of Ethylene. Polymerization of ethylene was carried out for complexes **3a**, **3b**, and **4b**. The results are summarized in Table 6. After activation with excess modified methylalumoxane, both **3a** and **3b** show marginal activity ($1-7 \times 10^4$ g of PE/mol$_{cat}$ atm h), and **4b** is not active for the polymerization. The activities of the diamidotitanium complexes are much lower than that of the titanocene complex (35×10^4 g of PE/mol$_{cat}$ atm h) measured under similar conditions (entry 7).

Although most polymer samples obtained from **3a** are not soluble even in refluxing 1,2,4-trichlorobenzene, measured T_ms are typical of high-density polyethylene (entries 1−3). When the polymerization is carried out at higher temperatures and with larger excesses of MAO, the activities marginally increase (entry 4). Polyethylenes obtained from **3b** seem to have low polydispersity (entry 5), probably because some portion of the polymer was washed away during the separation process due to its low molecular weight.

The polymerization behavior can be related to the alkylation process in the presence of MAO. No formation of bisalkylated product even with excess trimethylaluminum or triisobutylaluminum indicates that generation of bisalkylated species and cationic alkylated species is not easily achieved. This must be why the polymerization activity is generally low for the above cases. While facile monoalkylation was observed for both **3a** and **3b**, decomposition leading to formation of precipitate was the major pathway for **3a**. It is believed that formation of off-white insoluble polyethylene is associated with the decomposition. For **3b**, it can be speculated that sterically demanding tris(isopropylsilyl) groups on the rigid naphthalene link discourage the approach of ethylene to its coordination wedge. As a result, low molecular weight polyethylene was obtained.

Summary

Rigid diamido chelates, N,N′-disilylated 1,8-diaminonaphthalene, coordinate to generate mono(diamido)titanium and -zirconium dichlorides as well as a bis(diamido)zirconium complex. Whereas these metal chlorides are easily monoalkylated with trimethylaluminum or methylalumoxane, the corresponding bisalkylation is not accessible. It is believed that the resistance to form the bisalkylated products is associated with the low activity of the metal chlorides for the ethylene polymerization. Also, the transmetalation of the diamidotitanium dichloride produces a dinuclear aluminum complex.

Acknowledgment. This work is supported by the Korea Foundation of Science and Engineering (941-0300-035-1). The authors are grateful to Dr. Ki-Min Park and Mr. Jungseok Heo for X-ray crystallographic analysis.

Supporting Information Available: Tables S1−S20 listing full experimental details for data collection and refinement, atomic coordinates, bond distances and bond angles, and anisotropic displacement parameters (22 pages). Ordering information is given on any current masthead page.

OM980187R

---

(14) ^{1}H NMR data for [1,8-$C_{10}H_6(NSi(\mathit{i}\text{-}Pr)_3)_2$]Ti($CH_2CHMe_2$)Cl (toluene-$d_8$): δ 7.22 (d, 2H), 7.12 (t, 2H), 6.91 (d, 2H), 2.46 (m, Ti−$CH_2C\mathit{H}Me_2$), 1.93 (d, Ti−$C\mathit{H}_2CHMe_2$), 1.66 (sept, 6H), 1.15 (d, 18H), 1.10 (d, 18H), 0.88 (d, Ti−$CH_2CH\mathit{Me}_2$).